Exposure-Adjusted Bicycle Crash Risk Estimation and Safer Routing in Berlin

Eric Berger [*]   Edward Eichhorn [*]   Liaisan Faidrakhmanova [*]   Luise Grasl [*]   Tobias Schnarr [*]

Abstract

Accurately estimating the risk of bicycle crashes at street level requires consideration of both crash counts and cyclist exposure. However, exposure data from official counting stations is unavailable for most streets. This makes it difficult to identify streets that are dangerous. We therefore use Strava's bike trip data to estimate the relative crash risk across street segments and junctions in Berlin. We identify those with a higher or lower than expected occurrence of crashes, and enable a routing algorithm to suggest lower-risk routes.

1. Introduction

Cycling is far from a safe endeavour. 92,882 bicycle crashes were recorded in 2024, including 441 fatalities - 16% of all traffic deaths that year (Destatis, 2025). Yet it is rarely clear which streets are most dangerous and thus should be avoided by cyclists or made safer. Quantifying street-level danger is non-trivial because simple crash counts confound risk with exposure. Streets with high exposure, i.e. high numbers of cyclists, tend to accumulate more crashes even when per-cyclist risk is low (Lücken, 2018). Crashes must be normalised by cyclist counts; otherwise, dangerous streets can remain hidden in dense urban networks (Uijtdewilligen et al., 2024). Unfortunately, street-level cyclist counts are rare. Berlin, for example, provides hourly counts via official counting stations, but their limited coverage (20 stations for thousands of streets) makes them impractical for city-wide risk estimation (Senatsverwaltung für Mobilität, Verkehr, Klimaschutz und Umwelt). We address this problem by using bike trip counts from the fitness-tracking app Strava. These have been used to predict official bike counts (Dadashova et al., 2020). We show that they can serve as a proxy for cyclist exposure and estimate for all segments and junctions in Berlin's official cycling network relative risks (the ratio of observed to expected crashes).

---

[*]Equal contribution. Correspondence to: Tobias Schnarr <tobias-marco.schnarr@student.uni-tuebingen.de>.
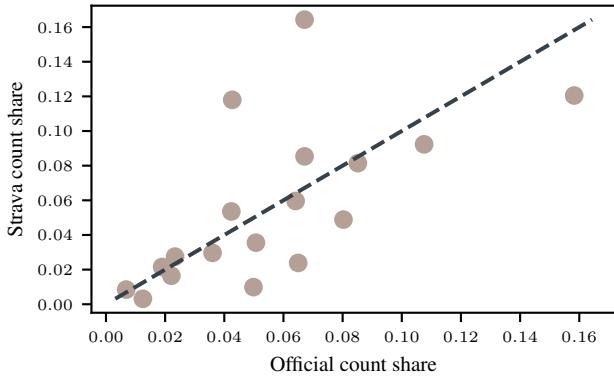
Because Strava coverage can be sparse, we use empirical Bayes smoothing for estimation (Clayton & Kaldor, 1987). This stabilises estimates for low-exposure segments and junctions, and quantifies uncertainty. We also introduce a routing algorithm that finds substantially lower-risk routes under a route-length constraint.

2. Data

Multiple datasets were used for risk estimation. Crash counts were taken from the *German Accident Atlas* (Destatis, 2025), which provides geodata of police-reported crashes where people were injured. We filtered the data to bicycle-related crashes within the city limits of Berlin. Cyclist exposure was approximated using the dataset by Kaiser et al. (2025b), which reports daily street-segment-level counts of bicycle trips recorded via the Strava app in Berlin from 2019 to 2023. Strava users are not representative of the general cycling population (they skew younger, male, and sport-oriented; Kaiser et al., 2025b). Therefore, we assess potential bias by comparing segment-level count shares in 2023 with official bicycle counter data from the city of Berlin (Senate Department for Urban Mobility, Transport, Climate Action and the Environment, 2024) for the subset of segments where both Strava and official counts are available (Figure 2). Count shares correlate strongly ($r = .61$) and are preserved in the Strava data. Segments on main streets where you can ride fast (e.g., Karl-Marx-Allee) are overrepresented in the Strava data, since those are more often tracked. Residential streets (e.g., Kollwitzstraße) are underrepresented, since slower, everyday cycling is less often tracked. All datasets were combined into one dataframe and matched to the same street network. The network is represented as segments with associated monthly exposure counts. We map crashes to the network using nearest-segment assignment. Junctions are defined as nodes where at least three segments meet and crashes within a fixed radius are assigned to the nearest junction. Junction exposure is derived from the segment exposure (see Section 3). At monthly resolution, events are sparse: in a typical month, fewer than 5% of segments and 3% of junctions record at least one crash. We drop segments with zero recorded trips over at least one year and pool counts over the full period 2019–2023 for risk estimation. The dataset comprises 4,335 segments, 2,862 junctions, and 15,396 recorded bicycle crashes.

(a) Data	(b) Risk estimation	(c) Safety routing

Figure 1. **Safety-aware routing pipeline for the Berlin network.** Panels (a–c) are zoomed in for readability; see Section 3 for definitions and notation. (a) Police-recorded bicycle crashes in June 2021 (points) and street segments with measured cyclist exposure (lines). (b) Pooled segment-level relative crash risk estimated from all available data; high-risk segments in red correspond to values above the 90th percentile of relative risk; circles mark junctions (degree ≥ 3). (c) Shortest path (blue) versus a safer alternative (green) selected to reduce cumulative relative route risk under a route-length constraint. Filled circle and cross denote origin and destination, respectively.


Figure 2. Consistency check between official bicycle counts and Strava bike trips at the street-segment level (2023). Points show segment-wise shares of total annual counts.

3. Methods

Crash, exposure, and risk measures. For each month t, let $C_{s,t}$ and $E_{s,t}$ denote the number of police-recorded bicycle crashes and measured cyclist exposure on street segment s. Junction crashes $C_{v,t}$ are defined as crashes within a fixed radius of junction v. Because a traversal typically contributes exposure to two incident segments, we approximate junction exposure by the half-sum of incident segment exposures,

$$E_{v,t} = \tfrac{1}{2} \sum_{s \in \mathcal{I}(v)} E_{s,t},$$

a common approach when turning movements are unavailable (Hakkert & Braimaister, 2002; Wang et al., 2020). For notational convenience, both street segments and junctions are indexed by a generic entity index i, with $A_{i,t}$ and $E_{i,t}$ denoting the corresponding crash and exposure quantities.

Under a no-special-risk baseline, monthly crash incidence

is assumed proportional to exposure, yielding the expected number of crashes

$$\widehat{C}_{i,t} = C_{\cdot t} \frac{E_{i,t}}{E_{\cdot t}}, \qquad C_{\cdot t} = \sum_i C_{i,t}, \ \ E_{\cdot t} = \sum_i E_{i,t},$$

where sums are taken jointly over all segments and junctions, defining a shared baseline. Because routing requires a pooled baseline risk estimate, crashes and baseline expectations are aggregated over the full period,

$$C_i = \sum_t C_{i,t}, \qquad \widehat{C}_i = \sum_t \widehat{C}_{i,t},$$

and the raw relative risk r_i^{raw} is $C_i / \widehat{C}_i$.

Empirical Bayes smoothing. Because many segments have low exposure and thus very small expected counts, the raw relative risk is highly variable. That is why we use Empirical Bayes smoothing to improve the risk estimates. This methods shrinks low-exposure estimates toward a baseline, while high-exposure estimates change little. Concretely, we assume a true relative risk r_i^{true} such that the observed count C_i follows a Poisson model with

$$C_i \mid r_i^{\mathrm{true}} \sim \mathrm{Poisson}(\widehat{C}_i \, r_i^{\mathrm{true}}).$$

The Poisson distribution is natural for nonnegative event counts over a fixed time period under a baseline rate, and it yields $\mathbb{E}[C_i] = \widehat{C}_i$ when $r_i^{\mathrm{true}} = 1$. To allow heterogeneity in relative risk beyond this baseline, we place a Gamma prior on r_i^{true} in the shape–rate parameterization,

$$r_i^{\mathrm{true}} \sim \mathrm{Gamma}(\alpha, \alpha),$$

which enforces $\mathbb{E}[r_i^{\mathrm{true}}] = 1$ and has variance $\mathrm{Var}(r_i^{\mathrm{true}}) = 1/\alpha$ controlling the amount of shrinkage. The Gamma prior is also conjugate to the Poisson likelihood, giving a closed-form posterior

$$r_i^{\mathrm{true}} \mid C_i, \widehat{C}_i \sim \mathrm{Gamma}(C_i + \alpha, \ \widehat{C}_i + \alpha),$$

so posterior inference is simple and numerically stable. We estimate α from the data using method of moments (Morris, 1983), as

$$\widehat{\alpha} = \frac{\sum_i \widehat{C}_i^2}{\sum_i (C_i - \widehat{C}_i)^2 - \sum_i \widehat{C}_i}.$$

and use the posterior mean

$$\widehat{r}_i = \mathbb{E}[r_i^{\text{true}} \mid C_i, \widehat{C}_i] = \frac{C_i + \alpha}{\widehat{C}_i + \alpha}$$

as the smoothed relative risk. For small $\widehat{C}_i$, r_i is pulled toward 1, while for large $\widehat{C}_i$ it approaches the raw ratio $C_i/\widehat{C}_i$. Uncertainty is summarized by $(1 - \delta = 0.95)$ equal-tailed credible intervals from quantiles of the Gamma posterior.

Risk-weighted routing graph. Relative risk estimates are dimensionless and conditional on exposure. To obtain additive routing weights, we rescale relative risk by the pooled baseline crash rate,

$$\bar{\lambda} = \frac{C.}{E.}, \qquad C. = \sum_i C_i, \;\; E. = \sum_i E_i,$$

yielding the routing weight

$$w_i = \bar{\lambda}\, r_i.$$

We construct an undirected graph $G = (V, E)$ from the street network, where nodes correspond to segment endpoints and edges to street segments of length ℓ_e. Each edge e corresponds to a segment s and inherits its weight, $w_e = w_s$. Junction identifiers and weights are mapped to nodes via spatial snapping in a projected coordinate system, producing a single risk-annotated network.

Safety-aware routing. We compare shortest-distance routes with alternatives that reduce estimated crash risk under a bounded detour. The length of a route P is

$$L(P) = \sum_{e \in P} \ell_e.$$

To incorporate segment- and junction-level risk, the risk contribution of edge $e = (u, v)$ is defined as

$$\rho_e = w_e + \eta\, \frac{w_u + w_v}{2},$$

where w_u and w_v denote junction routing weights (zero for non-junction nodes), yielding an additive surrogate for cumulative route risk.

For an origin–destination pair, the baseline route P_{dist} minimizes $L(P)$. The safety-aware route is obtained by solving

$$P_{\text{safe}} = \arg\min_P R(P) = \sum_{e \in P} \rho_e \tag{1}$$
$$\text{s.t. } L(P) \leq (1 + \varepsilon)\, L(P_{\text{dist}}),$$

where ε is the allowable relative detour (Ehrgott, 2005). We approximate this constraint using a weighted-sum sweep: for $\lambda \in \Lambda$,

$$P(\lambda) = \arg\min_P \left(\sum_{e \in P} \rho_e + \lambda \sum_{e \in P} \ell_e \right),$$

and select the feasible route minimizing $R(P)$. Shortest paths are computed using Dijkstra's algorithm (Dijkstra, 1959).

Evaluation metrics. For each origin–destination pair, we report the relative length increase

$$\Delta_L = \frac{L(P_{\text{safe}}) - L(P_{\text{dist}})}{L(P_{\text{dist}})}$$

and the relative risk reduction

$$\Delta_R = \frac{R(P_{\text{dist}}) - R(P_{\text{safe}})}{R(P_{\text{dist}})}.$$

Pairs with $R(P_{\text{dist}}) = 0$ are excluded from Δ_R. We additionally report the expected number of avoided crashes,
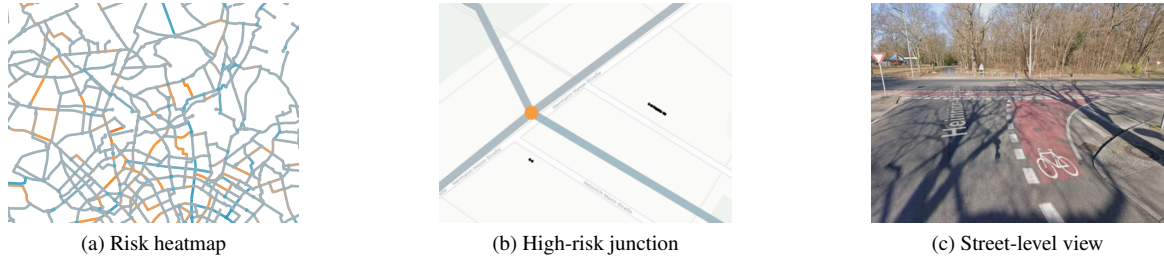
$$\Delta_C = R(P_{\text{dist}}) - R(P_{\text{safe}}).$$

4. Related Work

Prior studies combined police crash records with exposure estimates, but early work extrapolated bicycle traffic from motorized transport data, poorly capturing actual cycling patterns (Wage et al., 2022). Other work calibrated crowd-sourced GPS cycling data with count stations and showed that cyclist volumes predict crash risk, though uncertainty of risk estimates on low-volume segments remained unexamined (Uijtdewilligen et al., 2024; Medeiros et al., 2021). Where direct counts are unavailable, supervised learning and graph neural network approaches estimate city-wide volumes by combining sparse counters with crowdsourced data (Kaiser et al., 2025a;b). While these models required manual validation counts for calibration, they demonstrated that Strava data correlates with official counting stations at segment level, supporting its use as an exposure proxy. To account for accident sparsity, studies employed Poisson-Gamma count models (Lücken, 2018), but these remained limited to city-level aggregation, lacking segment-level estimates needed for routing applications.

5. Results

As described in Section 3, relative risk r_i was computed for each segment and junction. Due to high variance in the crash data, the shrinkage parameter was small ($\widehat{\alpha} = 0.129$), resulting in limited regularization and a wide spread

(a) Risk heatmap   (b) High-risk junction   (c) Street-level view

Figure 3. **Risk heatmap and detailed inspection of junction 2482.** Colors ▬▬▬▬ in panels (a) and (b) indicate $\log_{10}$-scaled relative risk values, ranging from low (-2) to high (2). (a) Zoomed-in view of the network showing estimated segment and junction risks. (b) Detailed view of junction 2482 with assigned crashes (black dots). (c) Street-level image of junction 2482 (Google, 2025), providing visual context for the observed risk.

of r_i estimates. These were mapped as partly shown in Figure 3(a). Most elements exhibit low risk: 64.4% of segments and 69.1% of junctions lie within the confidence bounds ($r_i = 1$). Values of $r_i < 1$ occur for 17.6% of segments and 25.8% of junctions, while 17.9% of segments and 4.9% of junctions show elevated risk ($r_i > 1$). Risk values range from 0.03–50.79 for segments and 0.03–6.43 for junctions. No overlap exists between the ten segments with the highest relative risk and those with the highest number of crashes. To verify that the method identifies high-risk locations, one such site was examined in detail. At junction 2482 ($r_i = 6.43$), 22 crashes occurred despite moderate traffic. All involved at least one additional vehicle - mostly cars (20) - and mainly resulted from turning or crossing maneuvers. As shown in Figure 3(c), car lanes intersect the bicycle lane at this junction. We evaluated the algorithm using 1,000 random origin–destination pairs, comparing the shortest-path baseline against safest alternatives across a range of allowable detour and junction-risk constraints (Natera Orozco et al., 2020).

Table 1. Trade-off between path length increase and safety improvement under varying detour budgets (ε). Values are aggregated over all origin–destination pairs and reported as medians. The junction penalty weight is fixed to $\eta = 1$. Δ_L denotes the relative path length increase, Δ_R the relative reduction in expected crashes with respect to the shortest-path baseline, and Δ_C the absolute number of avoided expected crashes per 100,000 trips, reported as rounded integer counts.

ε	Δ_L (IQR)	Δ_R (IQR)	$\Delta_R > 0$	Δ_C (IQR)
0.00	0.000 (0.000)	0.000 (0.000)	0.037	0 (0)
0.05	0.007 (0.022)	0.101 (0.210)	0.767	39 (123)
0.10	0.015 (0.037)	0.147 (0.240)	0.841	61 (132)
0.15	0.024 (0.063)	0.169 (0.239)	0.873	71 (141)
0.20	0.041 (0.109)	0.192 (0.238)	0.901	83 (150)
0.30	0.091 (0.156)	0.237 (0.228)	0.928	104 (157)
0.40	0.137 (0.188)	0.262 (0.230)	0.944	112 (170)
0.50	0.165 (0.200)	0.281 (0.222)	0.948	121 (178)

Table 1 summarizes the trade-off between route length and exposure-adjusted crash risk under bounded detours. With a strictly bounded detour of only 5%, the median risk reduction ranges between 18.5% and 24.6%, depending on the junction penalty. Larger detours further increase these gains, reaching median risk reductions of 38%-43% at $\varepsilon = 0.2$. Safer route alternatives are available for the vast majority of trips (76%–92%) within the given detour budget. As the budget increases to 20%, over 90% of routes have a feasible, lower-risk alternative. Across all detour budgets, increasing η is associated with lower median risk reductions.

6. Discussion and Conclusion

We developed a city-wide method for estimating bicycle crash risk using Strava exposure data. The approach enables safety-aware routing that balances crash risk reduction against route length constraints. Our approach faces two main limitations. First, official crash data capture only personal injury incidents and suffer from under-reporting, systematically underestimating absolute risk. Second, Strava data skew toward recreational rides on main roads, underrepresenting casual trips on residential streets. Where Strava overcounts exposure, calculated risk is too low; where it undercounts, sparse data yield inflated estimates. Empirical Bayes smoothing partially mitigates this by shrinking unstable low-exposure estimates toward the citywide baseline. Our junction exposure model assumes uniform flow and ignores turning movements. This misallocates exposure where one main road dominates side streets. Systematic biases in crowdsourced exposure data limit risk estimates' accuracy. While graph neural network methods can interpolate traffic volumes from sparse data (Kaiser et al., 2025b), they require manual validation counts. Cities with sparse counting networks like Berlin could address this by expanding automated counting infrastructure. Despite these limitations, the approach scales to any city with crash records and crowdsourced trip data, requiring only modest detours for

4

substantially safer routes.

Code and supplementary materials are available at https://github.com/ytobiaz/data_literacy.

Contribution Statement

Explain here, in one sentence per person, what each group member contributed. For example, you could write: Max Mustermann collected and prepared data. Gabi Musterfrau and John Doe performed the data analysis. Jane Doe produced visualizations. All authors will jointly wrote the text of the report. Note that you, as a group, a collectively responsible for the report. Your contributions should be roughly equal in amount and difficulty.

References

Clayton, D. and Kaldor, J. Empirical bayes estimates of age-standardized relative risks for use in disease mapping. *Biometrics*, 43(3):671, September 1987. ISSN 0006-341X. doi: 10.2307/2532003. URL http://dx.doi.org/10.2307/2532003.

Dadashova, B., Griffin, G. P., Das, S., Turner, S., and Sherman, B. Estimation of average annual daily bicycle counts using crowdsourced strava data. *Transportation Research Record: Journal of the Transportation Research Board*, 2674(11):390–402, September 2020. ISSN 2169-4052. doi: 10.1177/0361198120946016. URL http://dx.doi.org/10.1177/0361198120946016.

Destatis. German accident atlas, 2025. URL https://unfallatlas.statistikportal.de/. Retrieved January 14 2026.

Dijkstra, E. W. A note on two problems in connexion with graphs. *Numerische Mathematik*, 1(1):269–271, 1959. ISSN 0945-3245. doi: 10.1007/bf01386390. URL http://dx.doi.org/10.1007/BF01386390.

Ehrgott, M. *Multicriteria Optimization*, volume 491 of *Lecture Notes in Economics and Mathematical Systems*. Springer, Berlin, Heidelberg, 2005. ISBN 978-3-540-21398-7. URL https://doi.org/10.1007/3-540-27659-9.

Google. Google Street View: Junction Heinrich-Mann-Straße/Hermann-Hesse-Straße Berlin, 2025. URL https://maps.app.goo.gl/pxxqfSwW8Rbtu6AZ8.

Hakkert, A. S. and Braimaister, L. The uses of exposure and risk in road safety studies. Technical Report R-2002-12, SWOV Institute for Road Safety Research, Leidschendam, The Netherlands, 2002. URL http://www.swov.nl/rapport/R-2002-12.pdf.

Kaiser, S. K., Klein, N., and Kaack, L. H. From counting stations to city-wide estimates: data-driven bicycle volume extrapolation. *Environmental Data Science*, 4, 2025a. ISSN 2634-4602. doi: 10.1017/eds.2025.5. URL http://dx.doi.org/10.1017/eds.2025.5.

Kaiser, S. K., Rodrigues, F., Azevedo, C. L., and Kaack, L. H. Spatio-temporal graph neural network for urban spaces: Interpolating citywide traffic volume, 2025b. URL https://arxiv.org/abs/2505.06292.

Lücken, L. On the variation of the crash risk with the total number of bicyclists. *European Transport Research Review*, 10(2):33, 2018. doi: 10.1186/s12544-018-0305-9. URL https://doi.org/10.1186/s12544-018-0305-9.

Medeiros, R. M., Bojic, I., and Jammot-Paillet, Q. Spatiotemporal variation in bicycle road crashes and traffic volume in berlin: Implications for future research, planning, and network design. *Future Transportation*, 1(3):686–706, 2021. ISSN 2673-7590. doi: 10.3390/futuretransp1030037. URL https://www.mdpi.com/2673-7590/1/3/37.

Morris, C. N. Parametric empirical bayes inference: Theory and applications. *Journal of the American Statistical Association*, 78(381):47–55, 1983. ISSN 1537-274X. doi: 10.1080/01621459.1983.10477920. URL http://dx.doi.org/10.1080/01621459.1983.10477920.

Natera Orozco, L. G., Battiston, F., Iñiguez, G., and Szell, M. Data-driven strategies for optimal bicycle network growth. *Royal Society Open Science*, 7(12):201130, 2020. ISSN 2054-5703. doi: 10.1098/rsos.201130. URL http://dx.doi.org/10.1098/rsos.201130.

Senate Department for Urban Mobility, Transport, Climate Action and the Environment. Radverkehrszählstellen – jahresbericht 2023, 2024. URL https://www.berlin.de/sen/uvk/_assets/verkehr/verkehrsplanung/radverkehr/weitere-radinfrastruktur/zaehlstellen-und-fahrradbarometer/bericht_radverkehr_2023.pdf?ts=1752674590. Stand: 31.05.2024 (Berlin, Mai 2024). Accessed: 2026-02-01.

Senatsverwaltung für Mobilität, Verkehr, Klimaschutz und Umwelt. Zählstellen und fahrradbarometer: Fahrradverkehr in zahlen. URL https://www.berlin.de/sen/uvk/mobilitaet-und-verkehr/verkehrsplanung/radverkehr/weitere-radinfrastruktur/zaehlstellen-und-fahrradbarometer/.

Uijtdewilligen, T., Ulak, M. B., Wijlhuizen, G. J., Bijleveld, F., Geurs, K. T., and Dijkstra, A. Examining the crash risk factors associated with cycling by considering spatial and temporal disaggregation of exposure: Findings from four dutch cities. *Journal of Transportation Safety & Security*, 16(9):945–971, 2024.

doi: 10.1080/19439962.2023.2273547. URL https://doi.org/10.1080/19439962.2023.2273547.

Wage, O., Bienzeisler, L., and Sester, M. Risk analysis of cycling accidents using a traffic demand model. *The International Archives of the Photogrammetry, Remote Sensing and Spatial Information Sciences*, XLIII-B4-2022:427–434, 2022. doi: 10.5194/isprs-archives-XLIII-B4-2022-427-2022. URL https://isprs-archives.copernicus.org/articles/XLIII-B4-2022/427/2022/.

Wang, K., Zhao, S., and Jackson, E. Investigating exposure measures and functional forms in urban and suburban intersection safety performance functions using generalized negative binomial - p model. *Accident Analysis & Prevention*, 148:105838, 2020. ISSN 0001-4575. doi: https://doi.org/10.1016/j.aap.2020.105838. URL https://www.sciencedirect.com/science/article/pii/S0001457520316584.